of the aromatic ring is fast, and the protons in symmetrical positions on the rings are chemically equivalent (two AA'XX' systems). The high-field component of the X_c doublet of the cis conformer (Figure 7) is inverted selectively, as indicated by asterisks in Figure 9. (Actually, this inversion was not very clean, but nonideal behavior does not prevent one from separating z and zz order by the nonselective π pulse.) The zz order is transferred from the cis to the trans conformer and leads to antiphase doublets at the positions of the A_t and X_t resonances (Figure 7) in the zz-subspectrum. The transfer of z-magnetization leads to in-phase doublets at the same positions in the z-subspectrum. The migration of z-order through cis-trans exchange gives rise to an X_t doublet, while NOE within the cis conformer shows up as a small doublet of opposite sign at the A_c resonance position ($\omega_0\tau_c << 1$ in this system, hence positive NOE in 1D parlance). The increase of both the zz- and z-peaks with τ_m in Figure 9 is approximately linear for short mixing times. While the doublet of X_t increases with τ_m, the high-field signal, which stems from a superposition of the A_t and A_c doublets, shows a decay that is slower than that of the X_c doublet, since the A_c signal decreases while the A_t signal increases like the X_t signal. In the z-subspectrum extracted from the same data (which is equivalent to a conventional transient NOE difference spectrum), the exchange leads to positive X_t signals, while cross-relaxation leads to weak negative A_c signals. In systems where both mechanisms act simultaneously, the buildup of the signals in the zz-subspectrum yields direct information on the exchange rate, in analogy to 2D zz-spectroscopy.

Conclusions

The two examples discussed in this paper, i.e., the slow ring-flip of Tyr-35 in BPTI and the cis-trans isomerization in tyrosyl-proline, serve to illustrate the unique features of 1D and 2D zz-exchange spectroscopy. Future applications will not be restricted to such local molecular rearrangements. There is an abundance of dynamic systems where these methods can provide new insight, such as dynamic equilibria between native and denatured proteins or nucleic acids, between double- and single-stranded DNA fragments, electron exchange in redox-active proteins, chemical exchange in complexes formed between proteins and nucleic acids, or between biopolymers and low molecular weight effector or drug molecules.

Acknowledgment. The authors are indebted for stimulating discussions to Dr. M. H. Levitt. This work was supported in part by the Schweizerischer Nationalfonds (project 3.284.82) and the Kommission zur Förderung der wissenschaftlichen Forschung (projects 1120 and 1329).

Registry No. TyrPro, 51871-47-7; BPTI, 9087-70-1.

Interfacial Electron Transfer in TiO_2 Colloids

Graham T. Brown,[†] James R. Darwent,*[†] and Paul D. I. Fletcher[‡]

Contribution from the Department of Chemistry, Birkbeck College, University of London, London WC1E 7HX, United Kingdom, and the Department of Chemistry, University of Kent, Canterbury CT2 7NZ, United Kingdom. *Received February 15, 1985*

Abstract: Semiconductor colloids can be used to investigate the factors that control interfacial electron transfer. Such reactions are important in the design of new catalysts for photochemical reactions. Previous workers have shown that the surface charge on the particles will control the driving force for electron transfer. In this paper, the change in surface charge with pH is also shown to have a pronounced electrostatic effect on the rate of interfacial electron transfer from colloidal TiO_2 to ionic redox reagents such as methylviologen. The effect can be used to identify the point of zero ζ potential for TiO_2 colloids. The rate of electron transfer also depends on the surface area of the particles, so that larger particles react faster than smaller particles. Since colloids contain a discrete range of particle sizes, the kinetic rate profiles do not show simple monoexponential behavior. Instead the kinetics are characterized by an average rate constant, $\bar{k}_x$, and a parameter, ρ, which describes the spread of the distribution in particle sizes. The origin of this nonmonoexponential behavior was confirmed by applying the same analysis to both the kinetic data and particle size measurements obtained by dynamic laser light scattering for different TiO_2 colloids.

Electrostatic gradients at solid/liquid interfaces can be used to catalyze or direct competing chemical reactions. They are also important in electrochemistry and colloid science. Although semiconductor/liquid junctions have been extensively studied with macroscopic electrodes,[1-3] attention has only recently been focused on the photochemistry of transparent semiconductor colloids. These systems are well suited to time-resolved techniques such as flash photolysis,[4-14] fluorescence,[15-19] and resonance Raman spectroscopy.[20-23] They offer a valuable medium in which to study the parameters that determine interfacial electron transfer.

In colloids containing metal oxide particles, the pH of the solution and the surface area of the particles can control the rate of electron transfer to reagents such as methylviologen (MV^{2+}).[5,6,13,24] In general these colloids will contain particles with a discrete range of surface areas. The larger particles will react faster, so that nonmonoexponential kinetics should be expected. No discussion of this effect has so far appeared in the literature, although a general model for dispersed kinetics in heterogeneous systems was recently developed.[25] We have now

[†] University of London.
[‡] University of Kent. Present address: Department of Chemistry, University of Hull, Hull HU6 7RX, United Kingdom.

(1) Heller, A. *Science (Washington, D.C.)* **1984**, *223*, 1141.
(2) Bard, A. J. *J. Phys. Chem.* **1982**, *86*, 172.
(3) Grätzel, M. *Acc. Chem. Res.* **1981**, *14*, 376.
(4) Henglein, A. *Ber. Bunsen-Ges. Phys. Chem.* **1982**, *86*, 241.
(5) Duonghong, D.; Ramsden, J.; Grätzel, M. *J. Am. Chem. soc.* **1982**, *104*, 2977.
(6) Moser, J.; Grätzel, M. *J. Am. Chem. Soc.* **1983**, *105*, 6547; *Helv. Chim. Acta* **1982**, *65*, 1436; *J. Am. Chem. Soc.* **1984**, *106*, 6557.
(7) Bahnemann, D.; Henglein, A.; Lilie, J.; Spanhel, L. *J. Phys. Chem.* **1984**, *88*, 709.
(8) Bahnemann, D.; Henglein, A.; Spanhel, L. *Discuss. Faraday Soc.* **1984**, *78*.
(9) Kuczynski, J. P.; Milosavljevic, B. H; Thomas, J. K. *J. Phys. Chem.* **1984**, *88*, 980.
(10) Chandrasekaran, K.; Thomas, J. K. *J. Chem. Soc., Faraday Trans. 1* **1984**, *80*, 1163.
(11) Darwent, J. R. *J. Chem. Soc., Faraday Trans. 1* **1984**, *80*, 183.
(12) Brown, G. T.; Darwent, J. R. *J. Chem. Soc., Faraday Trans. 1*, **1984**, *80*, 1631.
(13) Brown, G. T.; Darwent, J. R. *J. Chem. Soc., Chem. Commun.* **1985**, 98.

0002-7863/85/1507-6446$01.50/0

tackled this problem by preparing two TiO_2 colloids with different average radii and different distributions about those average radii. When the results from dynamic laser light scattering[26,27] are compared with kinetic data, we find that nonexponential behavior is observed in both cases and this reflects the distribution of radii.

Grätzel et al. have shown that as the pH increases, the rate constants for interfacial electron transfer to viologens also increase.[5,6] This results from a cathodic shift in the potential of electrons on the particles, which increases the thermodynamic driving force for reaction. Similar effects have been observed in pulse radiolysis studies, where the electron transfer occurs in the opposite direction, i.e., from $MV^{+\cdot}$ to the particles.[24] We also reported this effect for electron transfer from TiO_2 colloids to oxygen and a zwitterionic electron acceptor, methyl orange.[12] However, for ionic electron acceptors an electrostatic effect can also be seen, as we reported in a preliminary communication.[13] This depends on the surface charge on the particles, which also changes with pH. It can be used to determine the point of zero ζ potential, where the pH is such that there is no net charge on the particles. It should be necessary to separate all three effects, i.e., electrostatic attraction, changes in overvoltage with pH, and the surface area of the particles, to provide a reliable comparison between different colloidal preparations.

Experimental Section

Microsecond flash photolysis experiments were performed with an Applied Photophysics K200 system using copper sulfate filters to remove excitation wavelengths below 290 nm and 10-cm quartz cells as described previously.[28] Preliminary laser flash photolysis studies were carried out at the SERC Laser Support Facility (Rutherford Appleton Laboratory) with an EMG 101E excimer laser operating with XeCl gas (308-nm emission, ca. 100 mJ per 15-ns pulse). Visible absorption spectra were recorded with a Perkin-Elmer 554 spectrophotometer using 1-cm quartz cells. Samples were outgassed by purging with O_2-free nitrogen for at least 30 min. Unless otherwise stated, all solutions contained TiO_2 (5×10^{-4} M), 0.1% polyvinyl alcohol (PVA) as a support and sacrificial electron donor, and 10^{-4} M methylviologen (MV^{2+}). The ionic strength was adjusted first with HCl and then the pH was increased with NaOH (10, 1, and 0.1 M) solutions. By starting at a low pH, the ionic strength of solution remains essentially unchanged as the pH increases.

PVA (M_r 72000) and MV^{2+} were supplied by BDH (AR grade). $TiCl_4$ (99%) was supplied by Aldrich and BDH. Water was double distilled. Two methods were used to form TiO_2 colloids. Method A was based on the preparation described by Henglein[4] and involved precipitation of TiO_2 by adding $TiCl_4$ (BDH) to aqueous ammonia. The ammonia was removed by filtration with washing and the slurry was peptized by boiling in HCl. Method B was as described by Grätzel and Moser.[6] $TiCl_4$ (Aldrich) was added dropwise to water in an ice bath. These colloids remained transparent and stable for months.

Particle sizes were determined by dynamic laser light scattering with the theory developed below and eq 3, 15, and 16. The radii refer to $\bar{r}_x$, so that the values include a correction which allows for the effect of the particle sizes on the amplitude of the scattering (eq 16). The measurements were made at the University of Kent with a goniometer constructed in that laboratory in combination with a Spectra Physics Model 168 2-W argon ion laser (operating at 488 nm), a Malvern K7025 correlator, and an EMI 9863 photomultiplier tube in a Malvern RR109 housing system. Sample solutions were filtered through Millipore 0.22-μm filters directly into Hellma fluorescence cells that were mounted in a transparent dish of toluene. Thermostating to ± 0.1 °C was achieved by circulating the toluene through an immersion coil in a Haake thermostat. Anomalously high scattering intensity "bursts" caused by the presence of dust in the sample were discriminated against and rejected by computer control of the instrument. The radii reported below refer to naked TiO_2 with no polymer support. There was less than a 5% spread in the radii of naked and PVA-coated particles, which suggests that the polymer did not significantly affect their diffusion coefficient. Particles prepared by method A had an average radius ($\bar{r}_x$) of 18 nm and those produced by method B had an average radius of 6 nm. Transmission electron microscopy (JEOL 200 CX) showed that the colloids contained roughly spherical particles.

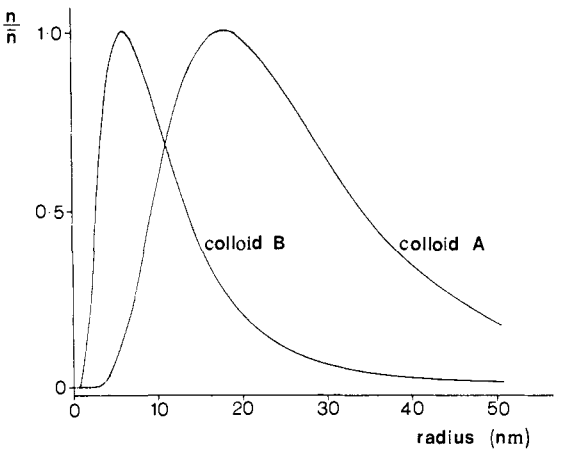

Figure 1. Distribution of particle sizes for colloid A ($\bar{r}_x$ = 18 nm, ρ = 0.6) and colloid B ($\bar{r}_x$ = 6 nm, ρ = 0.9).

Theory

Particle Size Effects. At least three factors can influence the rate of interfacial electron transfer from colloidal particles to redox agents in solution. These are the surface area of the particles, electrostatic attraction or repulsion between the charged particles and ionic reagents, and finally the thermodynamic driving force for electron transfer. In an analysis of transport and kinetics at microheterogeneous electrodes, Albery and Bartlett[29] showed that the effective second-order rate constant, k_E ($cm^3\ mol^{-1}\ s^{-1}$), was related to the electrochemical rate constant, k_{et} ($cm\ s^{-1}$), and the sum of the diffusion coefficients for the particles and reagents, D ($cm^2\ s^{-1}$) by eq 1

$$\frac{1}{k_E} = \frac{1}{4\pi r^2 L}\left(\frac{1}{k_{et}} + \frac{r}{D}\right) \tag{1}$$

where r (cm) is the radius of a particle and L (mol^{-1}) is Avogadro's number. For activation-controlled reactions where k_{et} is less than D/r, eq 1 will simplify to give

$$k_E = 4\pi r^2 L k_{et} \tag{2}$$

A similar approach was also developed by Grätzel and Frank for colloidal semiconductor particles and led to identical equations.[30]

Equation 2 suggests that the surface area will have a significant effect on the rate of interfacial electron transfer. An important result of this is that simple monoexponential kinetics should not be expected for electron-transfer reactions in semiconductor colloids. These colloids always contain a discrete distribution of particle radii around a mean value. Equation 2 shows that the

(14) Albery, W. J.; Brown, G. T.; Darwent, J. R.; Saievar-Iranizad, E. *J. Chem. Soc., Faraday Trans. 1* **1985**, *81*, 1999.
(15) Rossetti, R.; Brus, L. E. *J. Phys. Chem.* **1982**, *86*, 4470.
(16) Kuczynski, J. P.; Milosavljevic, B. H.; Thomas, J. K. *J. Phys. Chem.* **1983**, *87*, 3368.
(17) Weller, H.; Koch, U.; Gutiérrez, M.; Henglein, A. *Ber. Bunsen-Ges Phys. Chem.* **1984**, *88*, 649.
(18) Meyer, M.; Wallberg, C.; Kurihara, K.; Fendler, J. H. *J. Chem. Soc., Chem. Commun.* **1984**, 90.
(19) Grätzel, M.; Ramsden, J. *J. Chem. Soc., Faraday Trans. 1* **1984**, *80*, 919.
(20) Rossetti, R.; Beck, S. M.; Brus, L. E. *J. Am. Chem. soc.* **1984**, *106*, 980.
(21) Rossetti, R.; Brus, L. E. *J. Am. Chem. Soc.* **1984**, *106*, 4336.
(22) Rossetti, R.; Beck, S. M.; Brus, L. E. *J. Am. Chem. Soc.* **1982**, *104*, 7322.
(23) Metcalfe, K.; Hester, R. E. *J. Chem. Soc., Chem. Commun.* **1983**, 133.
(24) Dimitrijević, N. M.; Savić, D.; Mičić, O. I.; Nozik, A. J. *J. Phys. Chem.* **1984**, *88*, 4278.
(25) Albery, W. J.; Bartlett, P. N.; Wilde, C. P.; Darwent, J. R. *J. Am. Chem. Soc.* **1985**, *107*, 1854.
(26) Koppel, D. E. *J. Chem. Phys.* **1972**, *57*, 4814.
(27) Robinson, R. A.; Stokes, R. H. "Electrolyte Solutions"; Butterworth: London, **1959**; p 12.
(28) West, M. A. "Creation and Detection of Excited States"; Ware, W. R., Ed.; Marcel Dekker: New York, 1976; Vol. 4.
(29) Albery, W. J.; Bartlett, P. N. *J. Electroanal. Chem. Interfacial Electrochem.* **1982**, *131*, 137.
(30) Grätzel, M.; Frank, A. J. *J. Phys. Chem.* **1982**, *86*, 2964.

rate constant depends on r^2, so there will be a distribution of rate constants for the collection of particles and this will reflect the distribution of radii. Such an effect would account for the many examples of complex kinetics that have been reported for semiconductor colloids.[7,9,12-14,16-18]

In collaboration with Albery, Bartlett, and Wilde, we have developed a general model for dispersed kinetics in heterogeneous systems. This model is described in ref 25 and only points relevant to semiconductor colloids will be discussed here. One of the simplest distribution functions, which can be applied to colloids of this type, assumes that the number of particles (n) with a radius (r_x) is governed by a Gaussian function

$$n = \bar{n} \exp(-x^2) \tag{3a}$$

$$\rho x = \ln (r_x/\bar{r}_x) \tag{3b}$$

In these equations $\bar{r}_x$ and $\bar{n}$ are the number-average radius and the number of particles with the radius $\bar{r}_x$. This distribution function is described by two parameters: the number-average radius ($\bar{r}_x$) and the spread of the Gaussian (ρ). The shape of the distribution function is shown in Figure 1. Equation 2 suggests that this distribution of radii will lead to a range of rate constants, but the spread in the rate constants will be twice as large, since the rate constants are proportional to r^2, so that

$$\ln (k_x/\bar{k}_x) = 2\rho x \tag{4}$$

In this equation k_x (s^{-1}) is the pseudo-first-order rate constant for a particle with radius r_x. The rate constant is measured under reaction conditions where the reagent in solution (i.e., MV^{2+}) is in large excess, so that the reaction obeys a pseudo-first-order rate law. The total concentration of electrons on the particles (c) can be calculated at any time (t) by integrating over the normal distribution [$\exp(-x^2)$]

$$\frac{c}{c_0} = \frac{\int_{-\infty}^{+\infty} \exp(-x^2) \exp[-\tau \exp(\gamma x)]\, dx}{\int_{-\infty}^{+\infty} \exp(-x^2)\, dx} \tag{5}$$

where $\tau = \bar{k}_x t$ and $\gamma = 2\rho$.

When interfacial electron-transfer reactions are studied in photochemical systems by techniques such as flash photolysis, there is an additional complication to eq 5, since the larger particles will absorb more light during the photoflash. The absorption of light depends on the volume of the particles, and hence the normal distribution will be distorted in favor of the larger particles by $(r_x/\bar{r}_x)^3$. An attractive feature of this model for dispersal kinetics is that this factor can be easily allowed for by replacing x.[25] In this case the substitution is

$$z = x - 3\rho/2 \tag{6}$$

and so eq 5 becomes

$$\frac{c}{c_0} = \frac{\int_{-\infty}^{+\infty} \exp(-z^2) \exp[-\tau \exp(\gamma z)]\, dz}{\int_{-\infty}^{+\infty} \exp(-z^2)\, dz} \tag{7}$$

where $\tau = \bar{k}_z t$ and $\gamma = 2\rho$. Equation 7 retains the Gaussian shape, but now

$$\bar{k}_z = \bar{k}_x \exp(3\rho^2) \tag{8}$$

This equation reflects the fact that more electrons will be present immediately after the flash on larger particles where they react faster. Consequently the number-average rate constant per electron ($\bar{k}_z$) will be larger than the rate constant for a particle of average size ($\bar{k}_x$).

Effect of pH. The surface charge on colloidal oxide particles depends critically on pH. Any change in pH will lead to a variation in the surface charge, since protons and hydroxide ions will adsorb and desorb at the interface. In acidic media the particles carry a positive surface charge, but the charge decreases with increasing pH until a value is reached when the net charge is zero. This is known as the point of zero ζ potential (PZZP).[31] Above this pH the surface charge becomes increasingly negative. The adsorption and desorption of ions is a cooperative process, so that the variation in surface charge is thought to occur linearly over a wide pH range.[32] This change in surface charge will determine the electrochemical potential (E_p) of any electron on a particle

$$E_p = E_p^\circ + \frac{2.303RT}{F}(\text{PZZP} - \text{pH}) = E_p^\circ + 0.059(\text{PZZP} - \text{pH})V \tag{9}$$

In this equation E_p° is the electrochemical potential of an electron on a particle that has zero surface charge, i.e., at the pH of PZZP. Equation 9 is formally the same as that derived by Butler and Ginley for macroscopic oxide electrodes.[33]

The pH of PZZP can vary significantly for different oxide preparations. Values have been reported for TiO_2 ranging from 3.5 to 6.5.[34] This variation may result from entrapment of anions and cations during the particular preparation. Consequently at any pH eq 9 predicts that the reduction potential of an electron on TiO_2 particles could vary by as much as 180 mV for different preparations. This in turn will have a dramatic effect on the rate and yield of interfacial electron-transfer reactions.

In general the electrochemical rate constant, k_{et}, is expected to be related to the electrochemical driving force, $\eta(V)$, by a linear free energy relationship such as the Taffel equation[35]

$$\log k_{et} = \log k_{et}^\ominus + \frac{\alpha n F \eta}{2.303RT} \tag{10}$$

where n is the number of electrons transferred, $k_{et}^\ominus$ (cm s^{-1}) is the rate constant when η is zero, F is the Faraday constant, and α is the transfer coefficient. Here the overvoltage will be the difference between E_p and the standard reduction potential of the redox agent, $E_R(V)$

$$\eta = E_R - E_p \tag{11}$$

When eq 9–11 are combined we find

$$\log k_{et} = \log k_{et}^\circ + \alpha n(\text{pH} - \text{PZZP}) \tag{12}$$

Here k_{et}° (cm s^{-1}) is the electrochemical rate constant when the surface charge is zero

$$\log k_{et}^\circ = \log k_{et}^\ominus + \frac{\alpha n F}{2.303RT}(E_R - E_p^\circ) \tag{13}$$

This approach draws attention to the PZZP, whereas previous treatments have emphasized the pH at which the overvoltage will be zero.[6,30]

As well as changing the electrochemical potential, any pH variation will also affect the electrostatic charge that is experienced as an ionic reagent approaches a colloidal particle. At high ionic strength this effect will be negligible and eq 12 will apply, but in general eq 12 must be corrected to allow for variations in electrostatic attraction as the pH changes. For electron transfer from TiO_2 to MV^{2+} we find that α depends on the reciprocal of the square root of the ionic strength of the solution $I(M)$, so that

$$\alpha = \alpha_0 + z\beta/I^{1/2} \tag{14}$$

where $\beta M^{1/2}$ is a constant, which should depend on the rate of change of TiO_2 surface charge with pH, and z is the charge on the redox agent in solution (+2 for MV^{2+}). Also α_0 is the value of α when there is no electrostatic effect, i.e., at infinite ionic strength. The form of this equation is similar to that used in electrode kinetics to correct for variations in the potential drop across the electric double layer at moderate ionic strengths and

(31) Shaw, D. J. "Introduction to Colloid and Surface Science"; Butterworth: London, 1980.
(32) Ward, M. D.; White, J. R.; Bard, A. J. *J. Am. Chem. Soc.* **1983**, *105*, 27.
(33) Butler, M. A.; Ginley, D. S. *J. Electrochem. Soc.* **1978**, *125*, 228.
(34) Parks, G. A. *Chem. Rev.* **1965**, *65*, 177.
(35) Bard, A. J.; Faulkner, L. R. "Electrochemical Methods"; Wiley: New York, 1980.

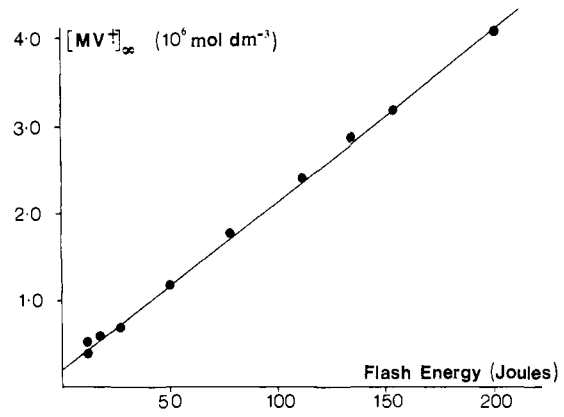

Figure 2. Variation in yield of $MV^{+\cdot}$ with light intensity (10^{-4} M MV^{2+}, 5×10^{-4} M TiO_2, 0.1 w/v % PVA).

low overvoltages.[35,36] This suggests that, in the pH range studied, the potential drop is due to ions in the diffuse double layer, rather than ions specifically adsorbed on the particles. At first sight this is surprising, since colloids are often stabilized by specific adsorption of ions. In this work, however, the particles were protected by steric stabilization[31] using PVA. In addition, this polymer may prevent the specific adsorption of ions. Also, the results in this work have focused on a narrow pH region close to the PZZP, where the charge on the particles will be relatively small. At high pH they will have a large negative surface charge and this will increase the likelihood of ions adsorbing on their surface.

Although eq 14 is a good empirical description in the pH region which we have investigated (pH 2–6), it may break down at high pH when the surface charge on the particles and the overvoltage for electron transfer are large. Particles with a high surface charge will bind counterions close to their surface and this may reduce the effective charge experienced by MV^{2+}.

Results and Discussion

Photosensitized reduction of MV^{2+} by TiO_2 colloids provides an excellent test system for the predictions of eq 7, 12, and 14. The redox properties of MV^{2+} are well-known and this dication should exhibit the electrostatic effects described by 14.

The principal reactions in this system are described in the following scheme:

$$TiO_2 + h\nu \rightarrow h + e \quad (I)$$

$$h + e \rightarrow \text{heat} \quad (II)$$

$$h + (PVA, H_2O) \rightarrow (\text{oxidized PVA, surface peroxide}) \quad (III)$$

$$MV^{2+} + e \rightarrow MV^{+\cdot} \quad (IV)$$

Absorption of light by TiO_2 creates an electron–hole pair (eh) in the semiconductor. The hole can react rapidly with PVA and water, so that after the 10-μs photoflash ($\lambda > 290$ nm) electrons are trapped on the particles. The subsequent electron transfer to MV^{2+} occurs on the microsecond and millisecond time scales and can be followed at 605 nm where $MV^{+\cdot}$ absorbs strongly.

This system has previously been investigated by the research groups of Grätzel and Henglein. There was some disagreement between the two groups about the rate profile for electron transfer. Grätzel et al. found that the reaction could be described by a monoexponential curve.[5,6] In contrast Henglein et al. found that the reaction was best described by a double-exponential function.[7] They attributed the slow phase of this process to electron transfer from a macroradical derived from the polymer PVA. In a preliminary communication, we also reported that the reaction was characterized by a double-exponential plot but attributed this to the dispersion in the radii of the particles.[13] The model for dispersed kinetics, developed above, should compare these possibilities. To test this we studied two different TiO_2 colloids, which had

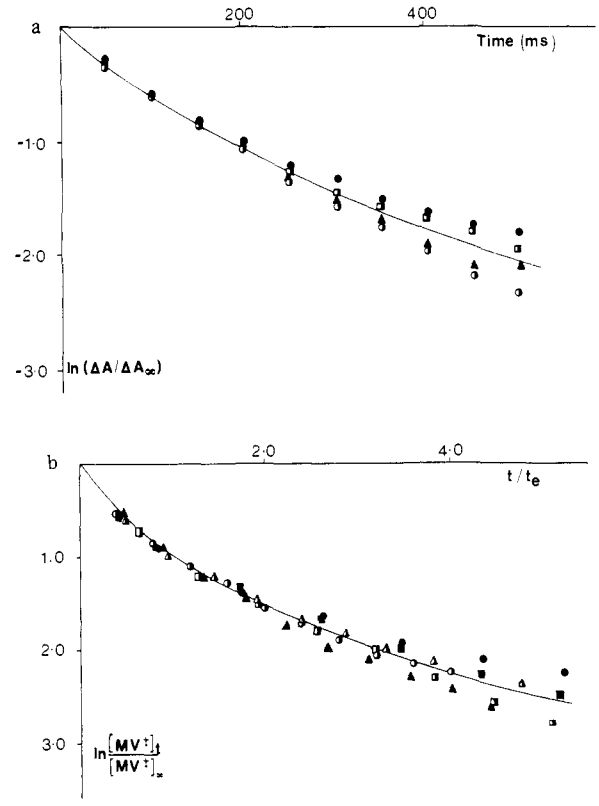

Figure 3. Typical time profiles for TiO_2 colloids, showing electron transfer to MV^{2+}. (a) For a range of flash intensity with the $r = 18$ nm colloid and final concentration of $MV^{+\cdot} = 0.4 \times 10^{-6}$ M (●), 1.2×10^{-6} M (◨), 2.4×10^{-6} M (◑), and 4.8×10^{-6} M (▲) and (b) for a range of pH and ionic strength values for the $r = 6$ nm colloid (▲) $I = 10^{-3}$ M, pH 4.3, $t_e = 1/k_z = 26$ ms; (△) $I = 10^{-3}$ M, pH 4.6, $t_e = 2.5$ ms; (■) $I = 10^{-3}$ M, pH 5.3, $t_e = 0.3$ ms; (◨) $I = 10^{-2}$ M, pH 3.1, $t_e = 250$ ms; (◑) $I = 10^{-1}$ M, pH 3.9, $t_e = 11$ ms; (●) $I = 10^{-1}$ M, pH 5.7, $t_e = 2.3$ ms.

different average radii and different ρ values.

When solutions of PVA (0.1% w/v), TiO_2 (5×10^{-4} M), and MV^{2+} (10^{-4} M) were flashed ($\lambda > 290$ nm), substantial concentrations of $MV^{+\cdot}$ were produced and the yield increased linearly with flash intensity (Figure 2). The flash energies refer to the total electrical energy, which is dissipated during the photoflash. This is composed largely of thermal and infrared radiation, which is absorbed by the copper sulfate filter solution and does not reach the sample. The figure suggests that oxidation of PVA (reaction III) competes effectively with charge recombination (reaction II). If this were not the case, the yield of $MV^{+\cdot}$ should increase with the square root of the light intensity, as recently observed in the photochemistry of CdS colloids.[14] For a typical flash intensity of 50 J an average of 500 electrons was trapped on each particle. The value was calculated from the concentration of $MV^{+\cdot}$ that was formed. This would correspond to a carrier density of ca. 10^{19} cm^{-3} and shows that in one photoflash the particles are transformed into heavily doped semiconductors. Insignificant (10^{-7} M) amounts of $MV^{+\cdot}$ were detected when no TiO_2 was present.

The kinetics of electron transfer were studied by following the absorption change at 605 nm due to the formation of $MV^{+\cdot}$. This process did not obey simple first-order kinetics (see Figure 3) and could be described equally well by a second-order or dual-exponential fit. In the case of the dual-exponential fit the weighting for the two processes was always about 1:1, and the ratio of the rate constants was 4:1 for the $r = 18$ nm colloid and 8:1 for the $r = 6$ nm particles. The weightings and ratios did not vary with pH.

This unusual behavior was not reported by Grätzel et al.,[5,6] although the kinetic traces in their publication suggest that the behavior was similar to that reported here.[5] Henglein et al. found similar complex behavior for electron transfer from TiO_2 to MV^{2+} and $C(NO_2)_4$ and fitted the kinetics to a dual-exponential function.[7] They attributed this to electron transfer from TiO_2 and

(36) Albery, W. J. "Electrode Kinetics"; Oxford University Press: London, 1975.

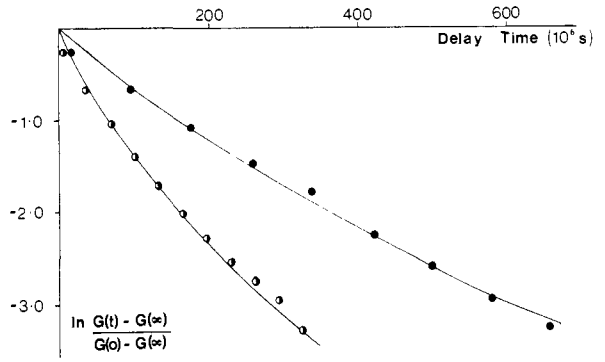

Figure 4. Decay of the autocorrelation function, $G(t)$, in dynamic light scattering experiments for TiO_2 colloids; r = 6 (◑) and r = 18 nm (●). The lines were calculated from eq 6 and 15 with ρ equal to 0.9 and 0.6, respectively.

from a macroradical derived from PVA. However, we find identical kinetic behavior for naked particles (pH 3) with no polymer support. These gave only 10% of the yield of $MV^{+\cdot}$, which is found when PVA is present, but the kinetic behavior was "biphasic" and had the same time constants as samples supported by PVA at the same pH. When no sacrificial electron donor, such as PVA, is present, photogenerated holes are thought to react at the surface of the particles to produce peroxides.[37,38] The low yield, in the absence of PVA, suggests that this is less effective than oxidation of PVA in competing with electron–hole recombination. These naked particles were only stable below pH 3.5 or above pH 9.0, so that it was not possible to follow the effect of changing pH with naked particles. The observation at pH 3, however, shows that both naked and PVA-coated particles had identical, complex, kinetic behavior. Thus the effect does not result from PVA. It seems likely that any PVA radicals will be strong reducing agents ($E_{1/2}$ for $(CH_3)_2\dot{C}OH$ is –0.86 V vs. NHE)[39] and should inject electrons into the TiO_2 to give a current doubling effect.

A more plausible explanation was presented above when we discussed the decay profile that is expected for an ensemble of particles with a distribution of radii. The model that we developed for a Gaussian distribution of radii predicts nonlinear ln (c/c_0) plots and can fit the data in Figure 3 with just two variables $\bar{k}_z$ and ρ. Figure 3a shows data for a wide range of flash intensities and hence a tenfold change in the concentration of $MV^{+\cdot}$ that is produced. All of the data fit on a common log (c/c_0) plot for the $\bar{r}_x$ = 18 nm colloid, which can be simulated with $\bar{k}_z$ and ρ equal to 5.0 s^{-1} and 0.55, respectively. This would not be possible if the reaction order was higher than 1. For example, if the reaction were second-order, then the initial half-life would drop by a factor of 10 since increasing the flash intensity leads in this experiment to a tenfold increase in the initial concentration of electrons on the particles.

Equivalent results were also obtained for the $\bar{r}_x$ = 6 nm colloid. Figure 3b shows typical results. In this case the results are shown for a range of ionic strengths and pHs. Again all the data fit a common curve with a constant ρ, although the value of $\bar{k}_z$ varies from 4.0 to 3300 s^{-1} as the ionic strength and pH are varied. This indicates that pH and ionic strength do not affect the width of the dispersion in rate constants, although changing the reaction conditions (pH and ionic strength) can increase the average rate constant by 3 orders of magnitude. The analysis also shows that the variations in pH and ionic strength do not change the effective radius ($\bar{r}_x$) or the distribution of the radii (ρ). The curves in Figure 3 show that the kinetics of these colloids can be described well by eq 7 where the curvature in the ln (c/c_0) plots result from a distribution of radii. In the case of the two colloids the values

(37) Brown, G. T.; Darwent, J. R. *J. Phys. Chem.* **1984**, *88*, 4955.
(38) Duonghong, D.; Grätzel, M. *J. Chem. Soc., Chem. Commun.* **1984**, 1597 and references therein.
(39) Lilie, J.; Beck, G.; Henglein, A. *Ber. Bunsen-Ges. Phys. Chem.* **1971**, *75*, 458.

Table I. Comparison of Radial Distribution from Dynamic Light Scattering and Kinetic Results

	ρ	
radius, nm	kinetic analysis	dynamic light scattering
18	0.55	0.6
6	0.9	0.9

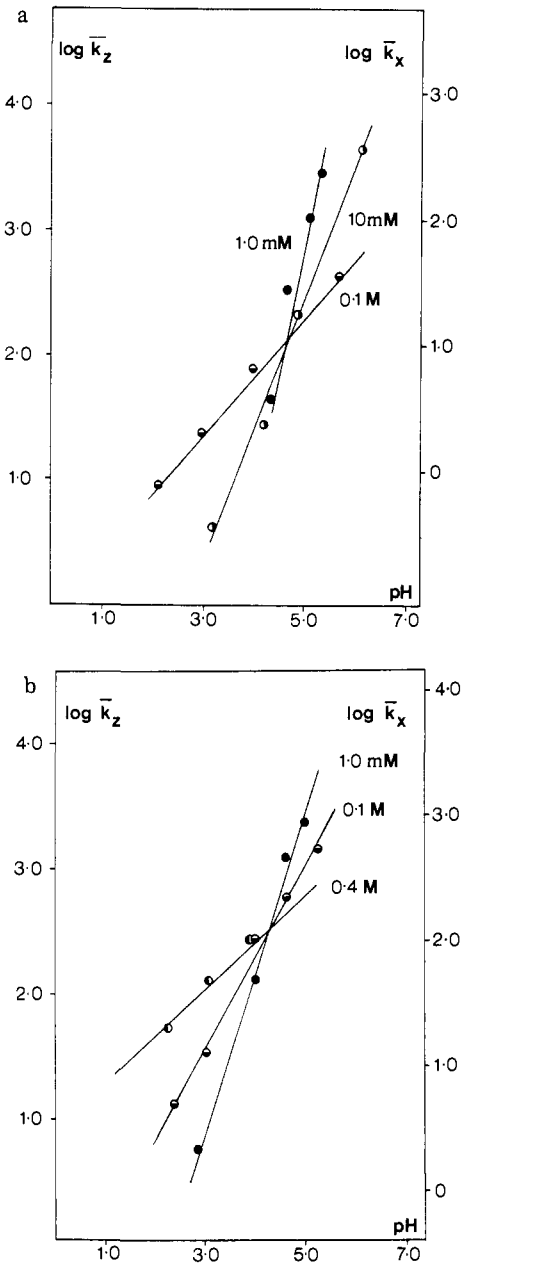

Figure 5. Variation in pseudo-first-order rate constants (k_x) for reduction of MV^{2+} (10^{-4} M) with pH and ionic strength; (a) $\bar{r}_x$ = 6 nm and (b) $\bar{r}_x$ = 18 nm. Ionic strength values are given on each line.

of ρ are 0.55 and 0.9 for the $\bar{r}_x$ = 18 and 6 nm colloids, respectively.

The distribution of radii can also be determined directly by dynamic laser light scattering. In this technique the diffusion coefficient D (m^2 s^{-1}) is calculated from the slope of a plot of the autocorrelation function against delay time.[26] Typical data for the two colloids are shown in Figure 4. An absolutely monodisperse collection of particles would give a straight line. In this case the same analysis can be applied to both the decay in autocorrelation function and the kinetic data. Since the diffusion coefficients[27] will be proportional to $1/r$, their distribution will be governed by eq 3 and hence

$$\ln D = \ln \bar{D} - \rho x \qquad (15)$$

Table II. Kinetic Parameters for Electron Transfer from TiO_2 to MV^{2+}

radius, nm	$\bar{k}_x$,[a] s^{-1}	PZZP	α_0	β	k_{et},[a] cm/s^{-1}
18 ± 1	180 ± 20	4.3 ± 0.1	0.5 ± 0.1	(2.0 ± 0.5) × 10^{-2}	(6 ± 2) × 10^{-5}
6.0 ± 0.5	10 ± 1.0	4.5 ± 0.1	0.45 ± 0.1	(2.0 ± 0.5) × 10^{-2}	(4 ± 1) × 10^{-5}

[a] Rate constants at PZZP for the respective colloid.

Since the larger particles scatter more light and diffuse more slowly, eq 5 will again be modified to give (16) where in this case $y = x + 3\rho/2$, $\gamma = -\rho$, and $\tau = 2K^2\bar{D}_y t$, where

$$\bar{D}_y = \bar{D}_x \exp(-3\rho^2/2) \quad (16)$$

and K is the scattering vector[26] (in this experimental system $K^2 = 5.9 \times 10^{-4}$ nm^2). The results for the two colloids are collected in Table I. This shows that there is excellent agreement between the spread of the Gaussian distributions (ρ values) which are obtained from the light scattering and kinetic measurements for the two sets of particles. Thus the light scattering confirms that the curvature in ln (c/c_0) plots is due to a distribution of radii. Interestingly the kinetic data are more sensitive to this distribution since the rate constants depend on r^2, whereas the diffusion coefficients are proportional to r^{-1}.

The analysis above shows that the rate of electron transfer can be characterized by an average rate constant, $\bar{k}_x$ (s^{-1}), and a parameter ρ, which describes the width of a Gaussian distribution of particle radii. Whereas ρ is a constant for a particular colloid, $\bar{k}_x$ is extremely sensitive to changes in the pH and ionic strength of the solution. This is shown clearly in Figure 5, parts a and b, which plot the value of log $\bar{k}_x$ against pH for a range of ionic strengths. The slope of log $\bar{k}_x$ against pH increased from 0.5 to 1.7 when the ionic strength was reduced from 0.1 to 10^{-3} mol dm^{-3} for the $r = 6$ nm particles. At low pH the rate was accelerated by a high ionic strength, which reduced electrostatic repulsion between MV^{2+} and the positively charged particles. This effect was then reversed at high pH where the particles carry a net negative charge. Both colloids show a unique pH value where the ionic strength has no effect on the rate. This will occur at their respective PZZPs when there will be zero charge on the particles.

Grätzel et al. have previously investigated the effect of pH on the rate of electron transfer to MV^{2+}.[5,6] They found the slope (α) was 0.48 for colloids prepared from titanium isopropoxide[5] and 0.85 for colloids prepared from $TiCl_4$;[6] however, they did not report the ionic strength at which their measurements were made. Here we find that α is proportional to $1/I^{1/2}$ and we have interpreted the data in Figure 5 with eq 12 and 14, using a multivariate linear least-squares analysis. The results of this analysis are collected in Table II. Both colloids have PZZPs close to the value of 4.7, which was measured by Grätzel et al. for a colloid of this type by conventional electrophoresis.[6] Normally electrophoresis is restricted to relatively large particles, since light scattering is used to follow the migration of charged particles in an electrostatic field.[40] In this study there is no such restriction since the kinetics reflect PZZPs for particles of all sizes.

The data in Figure 5 are derived from the Gaussian model and refer to particles with the average radius, i.e., $\bar{k}_x$. When a dual-exponential fit was used instead, identical values of α, β, and PZZP were obtained for both the slow and fast phases of the reaction. This is important, since it shows that the dispersion in the rate data (Figure 4) is not due to a dispersion in PZZP values. If there was a Gaussian distribution of PZZP values, then the slow phase of the reaction would have led to a lower mean PZZP value.

The values of α_0 and β are similar for the two colloids. The α_0 values are both close to 0.5 and show that a symmetrical transition state is involved in both reactions.[36] Identical values of β indicate that the change in surface charge density with pH is similar for the two preparations.

The average rate constants ($\bar{k}_x$) for the colloids at their PZZP values are very different (10 and 180 s^{-1}); however, this is expected from eq 2 since their average radii are also distinctly different. Allowing for the difference in their surface areas, eq 2 shows that the electrochemical rate constants are 4×10^{-5} and 6×10^{-5} cm s^{-1} for the $\bar{r}_x = 6$ and $\bar{r}_x = 18$ nm colloids at their respective PZZPs. These values are very similar, considering the uncertainty in the average radii and PZZP values. The difference in k_{et} is less than the experimental error. This result shows that eq 2 is indeed applicable to TiO_2 particles of this type and supports the kinetic analysis in terms of a dispersion of particle radii. Other workers have reported k_{et} values at the pH where the overvoltage is zero.[6,7] This is useful when the rate constants are compared with conventional electrochemical measurements. However, when comparing one colloidal preparation with another of the same material it may be helpful to compare k_{et} values at the PZZPs. Alternatively, it will be necessary to correct the k_{et} values at zero overvoltage for the difference in PZZPs and any differences in ionic strength.

Acknowledgment. We are grateful to Professor W. J. Albery for helpful discussions during the course of this work and to Dr. B. M. Robinson for help in measuring particle sizes. This research was supported by SERC and London University Central Research Fund. G.T.B. was supported by a CASE award from SERC and Unilever Research Ltd.

Registry No. MV^{2+}, 4685-14-7; TiO_2, 13463-67-7.

(40) Dunn, W. W.; Aikawa, Y.; Bard, A. J. *J. Am. Chem. Soc.* **1981**, *103*, 3456.